Chapter 7.3 Turbulent BL

Introduction: Transition to Turbulence

The transition process can be described as a succession of Tollmien-Schlichting waves, development of Λ - structures, vortex decay and formation of turbulent spots as preliminary stages to fully turbulent boundary-layer flow.

The phenomena observed during the transition process are similar for the flat plate boundary layer and for the plane channel flow, as shown in the following figure based on measurements by M. Nishioka et al. (1975). Periodic initial perturbations were generated in the BL using an oscillating cord.

For typical commercial surfaces transition occurs at $\mathrm{Re}_{x,tr} \approx 5 \times 10^5$. However, one can delay the transition to $\mathrm{Re}_{x,tr} \approx 3 \times 10^6$ with care in polishing the wall.
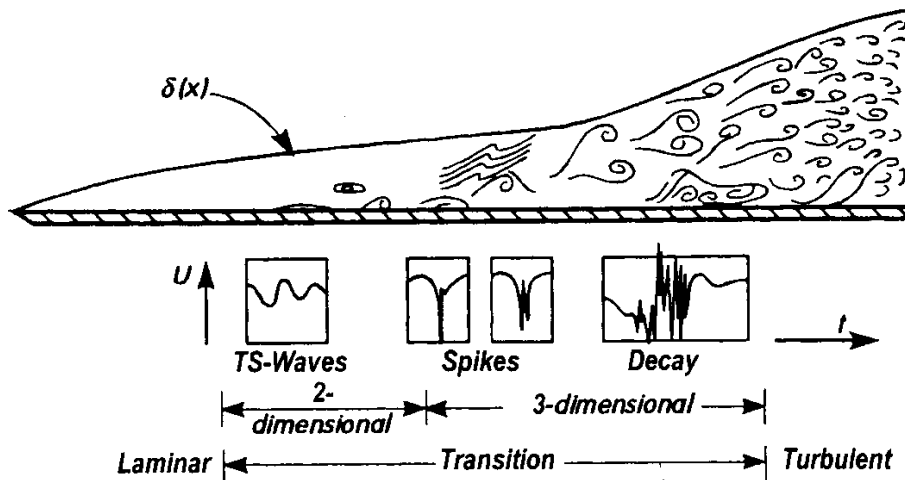

Fig. 15.38. Signals found at different regions in the transition at a plate at zero incidence, after M. Nishioka et al. (1975, 1990)

Reynolds Average of 2D boundary layer equations

$$u = \bar{u} + u'; \quad v = \bar{v} + v'; \quad w = \bar{w} + w'; \quad p = \bar{p} + p';$$

Substituting u, v and w into continuity equation and taking the time average we obtain,

$$\frac{\partial \bar{u}}{\partial x} + \frac{\partial \bar{v}}{\partial y} + \frac{\partial \bar{w}}{\partial z} = 0 \qquad \frac{\partial u'}{\partial x} + \frac{\partial v'}{\partial y} + \frac{\partial w'}{\partial z} = 0$$

Similarly, for the momentum equations and using continuity (neglecting g),

$$\rho \frac{D\bar{V}}{Dt} = -\nabla \bar{p} + \nabla \cdot \tau_{ij}$$

Where

$$\tau_{ij} = \mu \left(\frac{\partial u_i}{\partial x_j} + \frac{\partial u_j}{\partial x_i} \right) - \rho \overline{u_i' u_j'}$$

| Laminar | | Turbulent |

Assume

$$\delta(x) << x \text{ which means } \bar{v} << \bar{u}, \quad \frac{\partial}{\partial x} << \frac{\partial}{\partial y}$$

$$\text{mean flow structure is two-dimensional: } \bar{w} = 0, \quad \frac{\partial}{\partial z} = 0$$

Note the mean lateral turbulence is not zero, $\overline{w'^2} \neq 0$, but its z derivative is assumed to vanish.

Then, we get the following BL equations for incompressible steady flow:

$$\boxed{\frac{\partial \overline{u}}{\partial x} + \frac{\partial \overline{v}}{\partial y} = 0}$$ Continuity

$$\boxed{\overline{u}\frac{\partial \overline{u}}{\partial x} + \overline{v}\frac{\partial \overline{u}}{\partial y} \approx U_e \frac{dU_e}{dx} + \frac{1}{\rho}\frac{\partial \tau}{\partial y}}$$ x-momentum

$$\boxed{\frac{\partial p}{\partial y} \approx -\rho \frac{\partial \overline{v'^2}}{\partial y}}$$ y-momentum

Where U_e is the free-stream velocity and

$$\tau = \mu \frac{\partial \overline{u}}{\partial y} - \rho \overline{u'v'}$$

Note:
- The equations are solved for the time averages $\overline{u}$ and $\overline{v}$
- The shear stress now consists of two parts: 1. first part is due to the molecular exchange and is computed from the time-averaged field as in the laminar case; 2. The second part appears additionally and is due to turbulent motions.
- The additional term is new unknown for which a relation with the average field of the velocity must be constructed via a turbulence model.

Integrate y- momentum equation across the boundary layer

$$p \approx p_e(x) - \rho \overline{v'^2}$$

So, unlike laminar BL, there is a slight variation of pressure across the turbulent BL due to velocity fluctuations normal to the wall, which is no more than 4% of the stream-wise velocity and thus can be neglected.

The Bernoulli relation is assumed to hold in the inviscid free stream:

$$dp_e / dx \approx -\rho U_e dU_e / dx$$

Assume the free stream conditions, $U_e(x)$ is known, the boundary conditions:

No slip: $\bar{u}(x,0) = \bar{v}(x,0) = 0$

Free stream matching: $\bar{u}(x,\delta) = U_e(x)$

Flat plate boundary layer (zero pressure gradient)

$Re_t = 5 \times 10^5 \sim 3 \times 10^6$ for a flat plate boundary layer

$$Re_{crit} \sim 100,000$$

$$\frac{c_f}{2} = \frac{d\theta}{dx}$$

as was done for the approximate laminar flat plate boundary-layer analysis, solve by expressing $c_f = c_f(\delta)$ and $\theta = \theta(\delta)$ and integrate, i.e., assume log-law valid across entire turbulent boundary-layer

$$\frac{u}{u^*} = \frac{1}{\kappa} \ln \frac{yu^*}{\nu} + B$$

neglect laminar sub layer and velocity defect region

at $y = \delta$, $u = U$

$$\frac{U}{u^*} = \frac{1}{\kappa} \ln \frac{\delta u^*}{\nu} + B$$

$$Re_\delta \left(\frac{c_f}{2} \right)^{1/2}$$

or $\quad \left(\frac{2}{c_f} \right)^{1/2} = 2.44 \ln \left[Re_\delta \left(\frac{c_f}{2} \right)^{1/2} \right] + 5 \qquad \left.\begin{array}{c}\end{array}\right\} \quad c_f(\delta)$

$$c_f \cong .02 \, Re_\delta^{-1/6} \text{ power-law fit}$$

Next, evaluate

$$\frac{d\theta}{dx} = \frac{d}{dx} \int_0^\delta \frac{u}{U} \left(1 - \frac{u}{U} \right) dy$$

can use log-law or more simply a power law fit

$$\frac{u}{U} = \left(\frac{y}{\delta} \right)^{1/7} \qquad \left.\begin{array}{c}\end{array}\right.$$

Note: cannot be used to obtain $c_f(\delta)$ since $\tau_w \to \infty$

$$\theta = \frac{7}{72}\delta = \theta(\delta)$$

$$\Rightarrow \qquad \tau_w = c_f \frac{1}{2}\rho U^2 = \rho U^2 \frac{d\theta}{dx} = \frac{7}{72}\rho U^2 \frac{d\delta}{dx}$$

$$Re_\delta^{-1/6} = 9.72 \frac{d\delta}{dx}$$

or $\quad \dfrac{\delta}{x} = 0.16 \, Re_x^{-1/7}$

$$\delta \propto x^{6/7} \quad \text{almost linear}$$

i.e., much faster growth rate than laminar boundary layer

$$c_f = \frac{0.027}{\text{Re}_x^{1/7}}$$

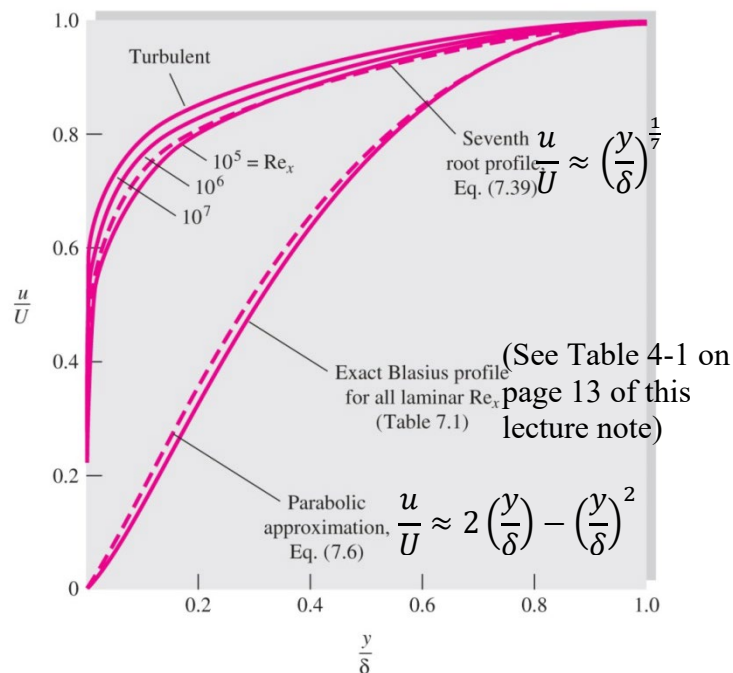$$\tau_{w,turb} = \frac{0.0135 \mu^{1/7} \rho^{6/7} U^{13/7}}{x^{1/7}}$$

$\tau_{w,turb}$ decreases slowly with x, increases with ρ and U^2 and insensitive to μ

$$C_D = C_f = \frac{0.031}{Re_L^{1/7}} = \frac{7}{6} c_f(L)$$

$$\delta^* = \frac{1}{8}\delta$$

$$H = \frac{\delta^*}{\theta} = 1.3$$

These formulas are for a fully turbulent flow over a smooth flat plate from the leading edge; in general, give better results for sufficiently large Reynolds number $Re_L > 10^7$.

Comparison of dimensionless laminar and turbulent flat-plate velocity profiles (Ref: White, F. M., Fluid Mechanics, 7th Ed., McGraw-Hill)

Alternate forms by using the same velocity profile $u/U = (y/\delta)^{1/7}$ assumption but using an experimentally determined shear stress formula $\tau_w = 0.0225\rho U^2(v/U\delta)^{1/4}$ are:

$$\frac{\delta}{x} = 0.37\,\mathrm{Re}_x^{-1/5} \qquad c_f = \frac{0.058}{\mathrm{Re}_x^{1/5}} \qquad C_f = \frac{0.074}{\mathrm{Re}_L^{1/5}}$$

shear stress: $\tau_w = \dfrac{0.029\rho U^2}{\mathrm{Re}_x^{1/5}}$

These formulas are valid only in the range of the experimental data, which covers $\mathrm{Re}_L = 5 \times 10^5 \sim 10^7$ for smooth flat plates.

Other empirical formulas are by using the logarithmic velocity-profile instead of the 1/7-power law:

$$\frac{\delta}{L} = c_f(0.98 \log Re_L - 0.732)$$

$$c_f = (2 \log Re_x - 0.65)^{-2.3}$$

$$C_f = \frac{0.455}{(\log_{10} Re_L)^{2.58}}$$

These formulas are also called as the *Prandtl-Schlichting skin-friction formula* and valid in the whole range of $\mathrm{Re}_L \leq 10^9$.

For these experimental/empirical formulas, the boundary layer is usually "tripped" by some roughness or leading-edge disturbance, to make the boundary layer turbulent from the leading edge.

No definitive values for turbulent conditions since depend on empirical data and turbulence modeling.

Finally, composite formulas that consider both the initial laminar boundary layer and subsequent turbulent boundary layer, i.e., in the transition region ($5 \times 10^5 < \text{Re}_L < 8 \times 10^7$) where the laminar drag at the leading edge is an appreciable fraction of the total drag:
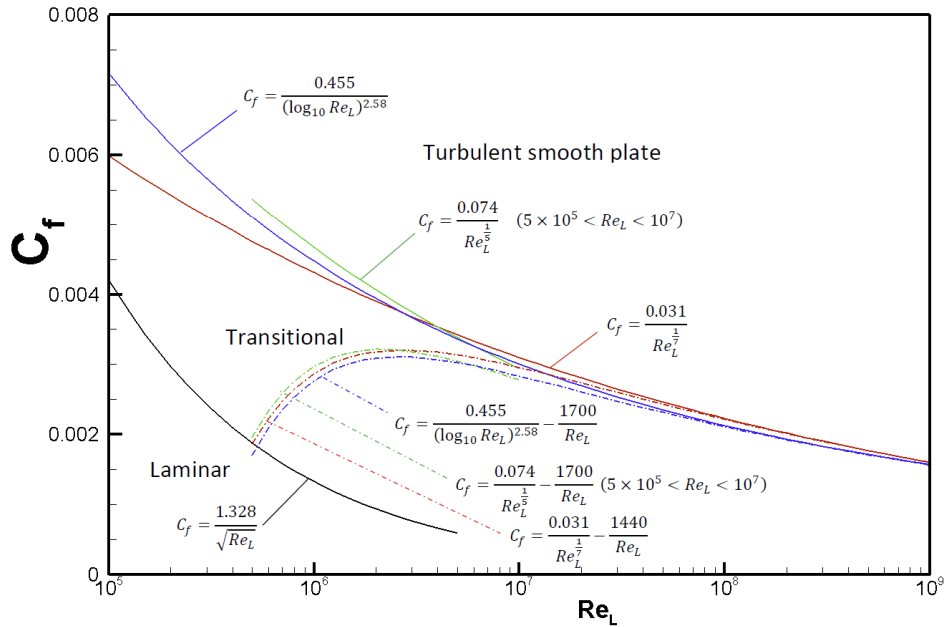
$$C_f = \frac{0.031}{Re_L^{\frac{1}{7}}} - \frac{1440}{Re_L}$$

$$C_f = \frac{0.074}{Re_L^{\frac{1}{5}}} - \frac{1700}{Re_L}$$

$$C_f = \frac{0.455}{(\log_{10} Re_L)^{2.58}} - \frac{1700}{Re_L}$$

with transitions at $\text{Re}_t = 5 \times 10^5$ for all cases.
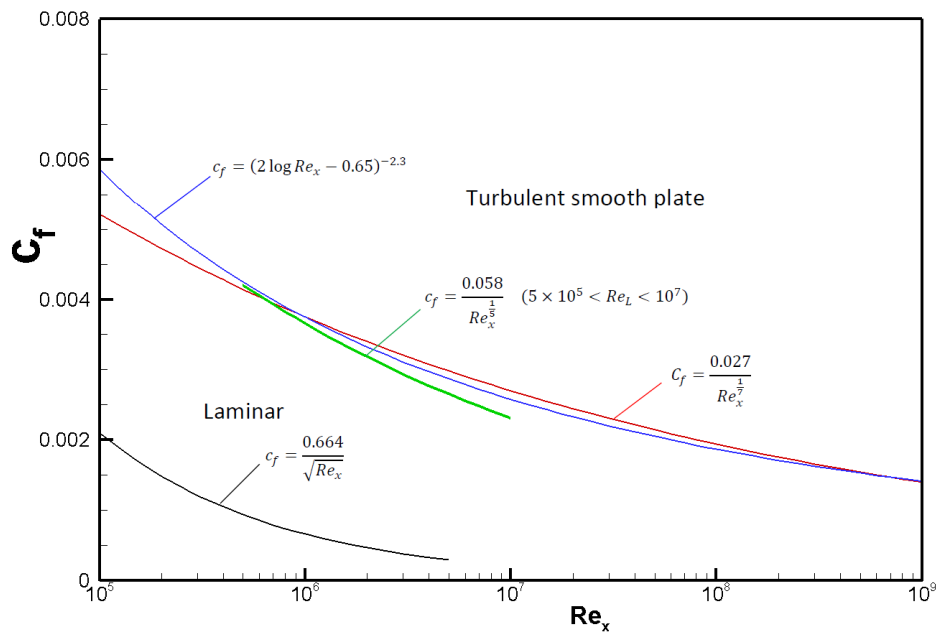
Local friction coefficient c_f (top) and friction drag coefficient C_f (bottom) for a flat plate parallel to the upstream flow.
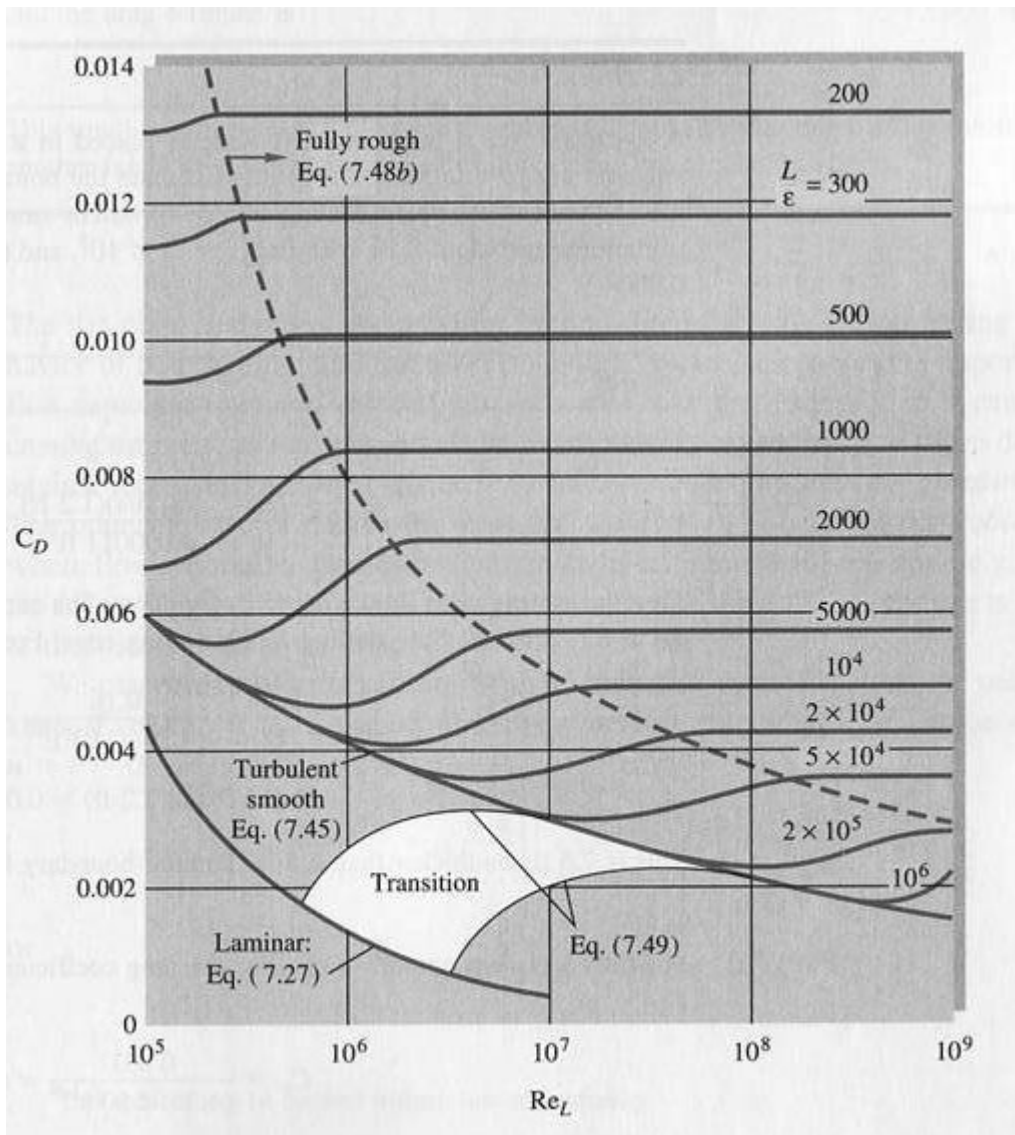
Fig. 7.6 Drag coefficient of laminar and turbulent boundary layers on smooth and rough flat plates.

$$C_f = (2.87 + 1.58 \log \frac{x}{\varepsilon})^{-2.5}$$

$$C_D = (1.89 + 1.62 \log \frac{L}{\varepsilon})^{-2.5}$$

Fully rough flow

Again, shown on Fig. 7.6. along with transition region curves developed by Schlichting which depend on $Re_t = \begin{cases} 5 \times 10^5 \\ 3 \times 10^6 \end{cases}$

Momentum Integral Equations valid for BL solutions

The momentum integral equation has the identical form as the laminar-flow relation:

$$\frac{d\theta}{dx} + (2+H)\frac{\theta}{U_e}\frac{dU_e}{dx} = \frac{\tau_w}{\rho U_e^2} = \frac{C_f}{2}$$

For laminar flow:

(C_f, H, θ) are correlated in terms of simple parameter $\quad \lambda = \frac{\theta^2}{\upsilon}\frac{dU_e}{dx}$

For Turbulent flow:

(C_f, H, θ) cannot be correlated in terms of a single parameter. Additional parameters and relationships are required that model the influence of the turbulent fluctuations. There are many possibilities all of which require a certain amount of empirical data. As an example, we will review the π–β method.

π-β *Method*

As mentioned earlier, the momentum integral equation for turbulent flow has the identical form as the laminar-flow relation:

$$\frac{d\theta}{dx} = \frac{C_f}{2} - (2+H)\frac{\theta}{U_e}\frac{dU_e}{dx} \qquad \text{(I)}$$

With U(x) assumed known, there are three unknown C_f, H, θ for turbulent flow. Thus, at least two additional relations are needed to find unknowns. There are many possibilities for additional relations all of which require a certain amount of empirical data. As an example we will review the π-β method.

Cole's law of the wake:
By adding the wake to the log-law, the velocity profile for both overlap and outer layers can be written as:

$$u^+ = \frac{1}{\kappa}\ln y^+ + B + \frac{2\Pi}{\kappa}f(\eta)$$

where

$$\eta = y/\delta$$

$$f(\eta) = \sin^2(\frac{\pi}{2}\eta) = 3\eta^2 - 2\eta^3$$

$$\Pi = \kappa A/2$$

The quantity Π is called Coles' wake parameter.

By integrating wall-wake law across the boundary layer:

$$\lambda = a(\Pi)\frac{H}{H-1}$$

$$a(\Pi) = \frac{2 + 3.179\Pi + 1.5\Pi^2}{\kappa(1+\Pi)}$$

$$\text{Re}_\theta = \frac{U\theta}{\upsilon} = \frac{1+\Pi}{\kappa H}\exp(\kappa\lambda - \kappa B - 2\Pi)$$

If we eliminate Π between these formulas, we obtain a unique relation among $C_f = 2/\lambda^2$, H and θ:

$$
\begin{cases}
C_f = 2/\lambda^2 = 2/[a(\Pi)\dfrac{H}{H-1}]^2 \\[2mm]
a(\Pi) = \dfrac{2+3.179\Pi+1.5\Pi^2}{\kappa(1+\Pi)} \\[2mm]
Re_\theta = \dfrac{U\theta}{\upsilon} = \dfrac{1+\Pi}{\kappa H}\exp(\kappa\lambda - \kappa B - 2\Pi)
\end{cases}
\qquad\text{(II)}
$$

Clauser's equilibrium parameter β:

For outer layer,
$$U_e - \bar{u} = f(\tau_w, \rho, y, \delta, \frac{dp}{dx})$$

Using dimensional analysis:
$$\frac{U_e - \bar{u}}{(\tau_w/\rho)^{1/2}} = g(\frac{y}{\delta}, \frac{\delta}{\tau_w}\frac{dp}{dx})$$

Clauser (1954) replaced δ by displacement thickness δ^*:
$$\frac{U_e - \bar{u}}{(\tau_w/\rho)^{1/2}} = g(\frac{y}{\delta}, \beta)$$

$$\beta = \frac{\delta^*}{\tau_w}\frac{dp}{dx} = -\lambda^2 H\frac{\theta}{U_e}\frac{dU_e}{dx}$$

β is called Clauser's equilibrium parameter.

Das (1987) showed that EFD data points fit into the following polynomial correlation:
$$\beta = -0.4 + 0.76\Pi + 0.42\Pi^2$$

Therefore:
$$-\lambda^2 H\frac{\theta}{U_e}\frac{dU_e}{dx} = -0.4 + 0.76\Pi + 0.42\Pi^2 \qquad\text{(III)}$$

If we eliminate Π using that $\mathrm{Re}_\theta = \dfrac{U\theta}{\upsilon} = \dfrac{1+\Pi}{\kappa H}\exp(\kappa\lambda - \kappa B - 2\Pi)$, we obtain another relation among $C_f = 2/\lambda^2$, H and θ.

Equations (I), (II), and (III) can be solved simultaneously using say a Runge-Kutta method to find C_f, H, θ. Equations are solved with initial condition for $\theta(x_0)$ and integrated to $x=x_0+\Delta x$ iteratively. Estimated θ gives Re_θ and Π, β gives H. Lastly C_f is evaluated using Re_θ and H. Iterations required until all relations satisfied and then proceed to next Δx.

Separation

The increasing downstream pressure slows down the wall flow and can make it go backward-flow separation.

$dp/dx > 0$ adverse pressure gradient, flow separation may occur.

$dp/dx < 0$ favorable gradient, flow separation can never occur

Previous analysis of BL was valid before separation.
Separation Condition

$$\tau_w = \mu\left(\frac{\partial u}{\partial y}\right)_{y=0} = 0$$
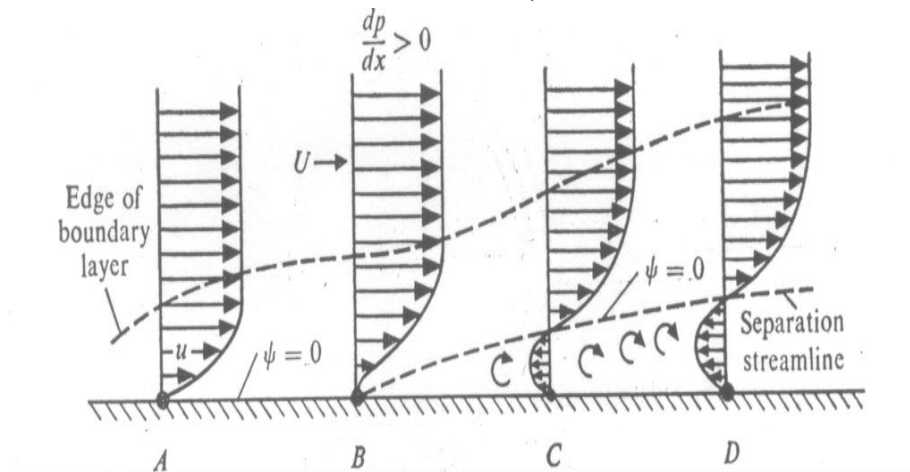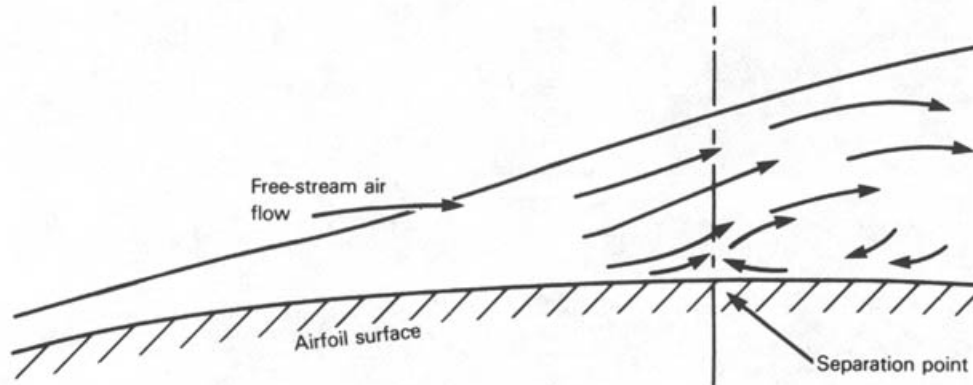
Note: 1. Due to backflow close to the wall, a strong thickening of the
        BL takes place and BL mass is transported away into the

   2. At the point of separation, the streamlines leave the wall at a
      certain angle.

Separation of Boundary Layer
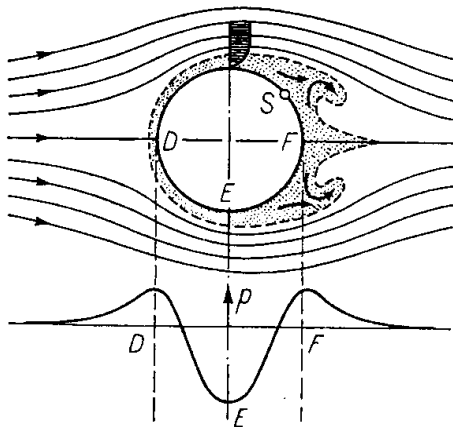
Fig. 2.6. Separation of the boundary layer
and vortex formation at a circular cylinder
(schematic). S = separation point

Notes:
1. D to E, pressure drop, pressure is transformed into kinetic energy.

3. A fluid particle directly at the wall in the boundary layer is also
   acted upon by the same pressure distribution as in the outer flow
   (inviscid).
4. Due to the strong friction forces in the BL, a BL particle loses so
   much of its kinetic energy that is cannot manage to get over the
   "pressure gradient" from E to F.
5. The following figure shows the time sequence of this process:
   a. reversed motion begun at the trailing edge

b. boundary layer has been thickened, and start of the reversed motion has moved forward considerably.

c. and d. a large vortex formed from the backflow and then soon separates from the body.
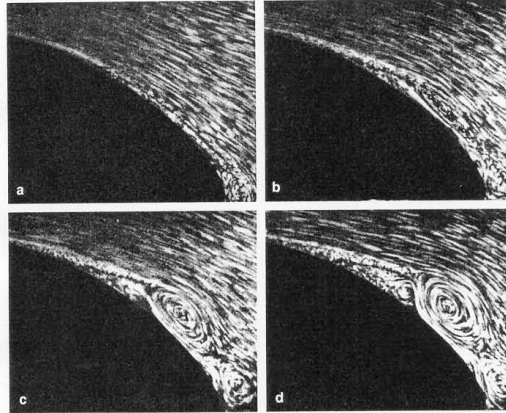
Fig. 2.7 a-d.   Development in time of the separation at the back of a blunt body, after L. Prandtl; O. Tietjens (1931)

Examples of BL Separations (two-dimensional)

Features: The entire boundary layer flow breaks away at the point of zero wall shear stress and, having no way to diverge left or right, has to go up and over the resulting separation bubble or wake.

1. Plane wall(s)

Thin wall
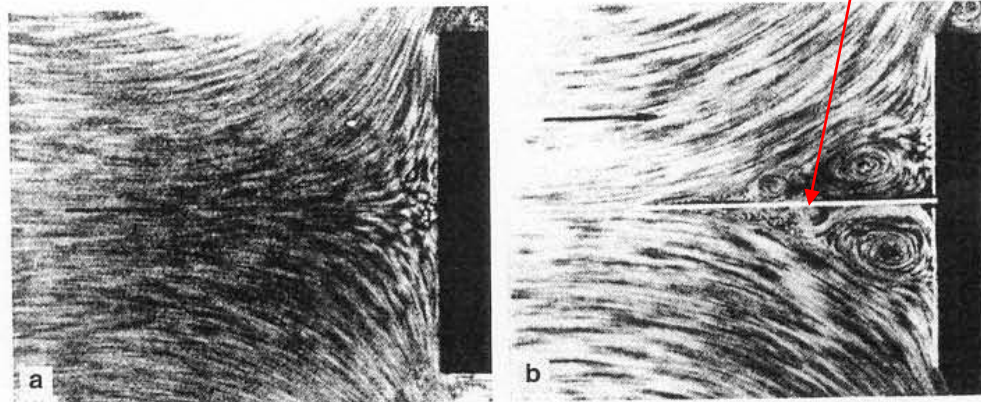
Fig. 2.10.   Stagnation point flow, after H. Föttinger (1939), (a) free stagnation–point flow without separation, (b) retarded stagnation–point flow, with separation

(a). Plane stagnation-point flow: no separation on the streamlines of symmetry (no wall friction present), and no separation at the wall

(b). Flat wall with right angle to the wall: flow separate, why?

2. Diffuser flow:
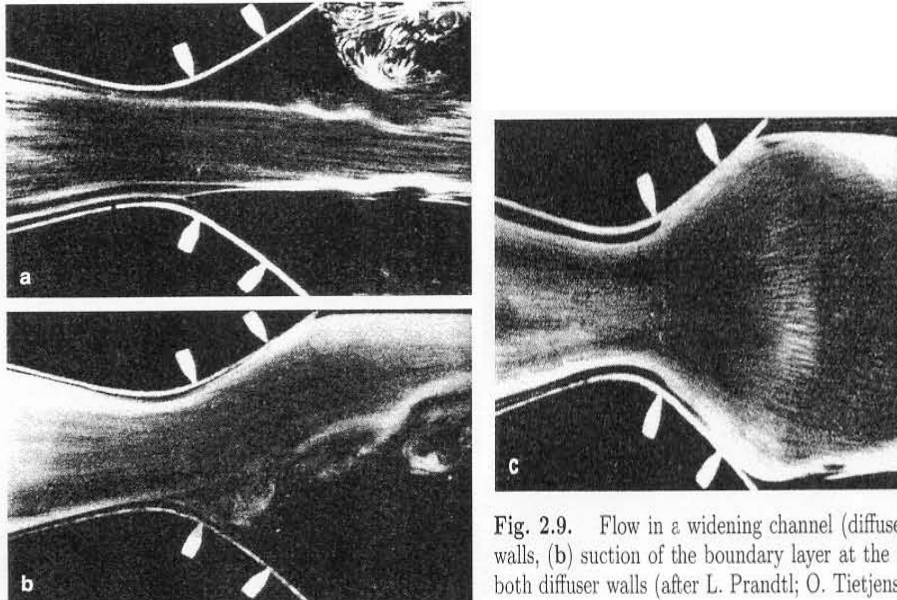
Fig. 2.9. Flow in a widening channel (diffuser) (a) separation at both diffuser walls, (b) suction of the boundary layer at the upper diffuser wall, (c) suction at both diffuser walls (after L. Prandtl; O. Tietjens (1931))

3. Turbulent Boundary Layer

(a)

(b)
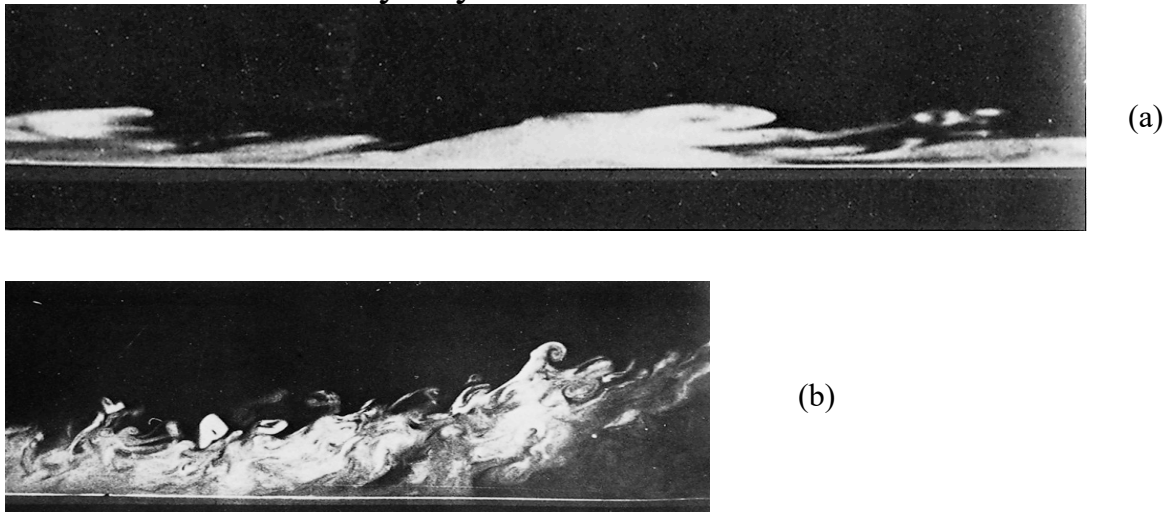
Influence of a strong pressure gradient on a turbulent flow
(a) a strong negative pressure gradient may re-laminarize a flow
(b) a strong positive pressure gradient causes a strong boundary
    layer top thicken. (Photograph by R.E. Falco)

Examples of BL Separations (three-dimensional)
    Features: unlike 2D separations, 3D separations allow many more
options.
    There are four different special points in separation:
    (1). *A nodal Point*, where an infinite number of surface streamlines

merged tangentially to the separation line

(2). *A saddle point*, where only two surface streamlines intersect and all others divert to either side

(3). *A focus, or spiral node*, which forms near a saddle point and around which an infinite number of surface streamlines swirl

(4). *A three-dimensional singular point*, not on the wall, generally serving as the center for a horseshoe vortex.

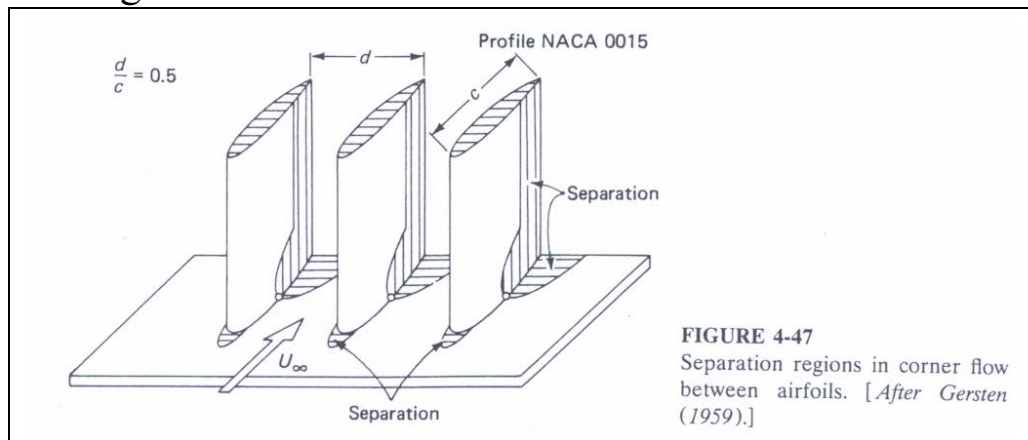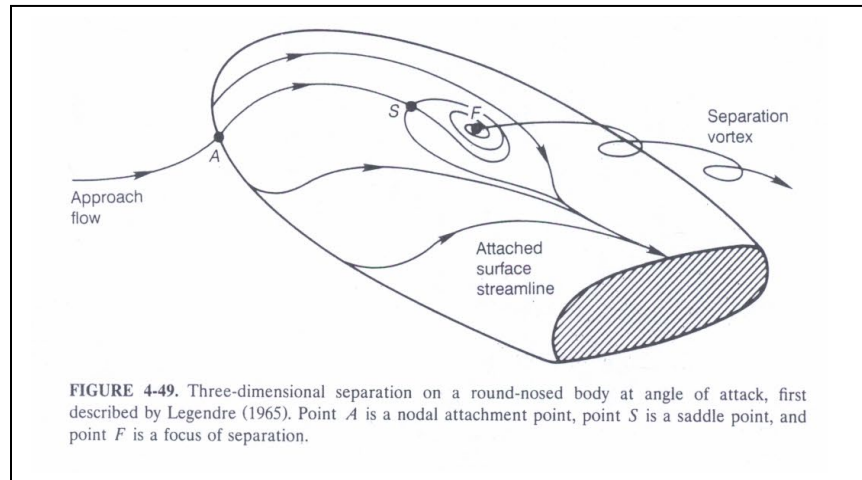1. Boundary layer separations induced by free surface (animation)
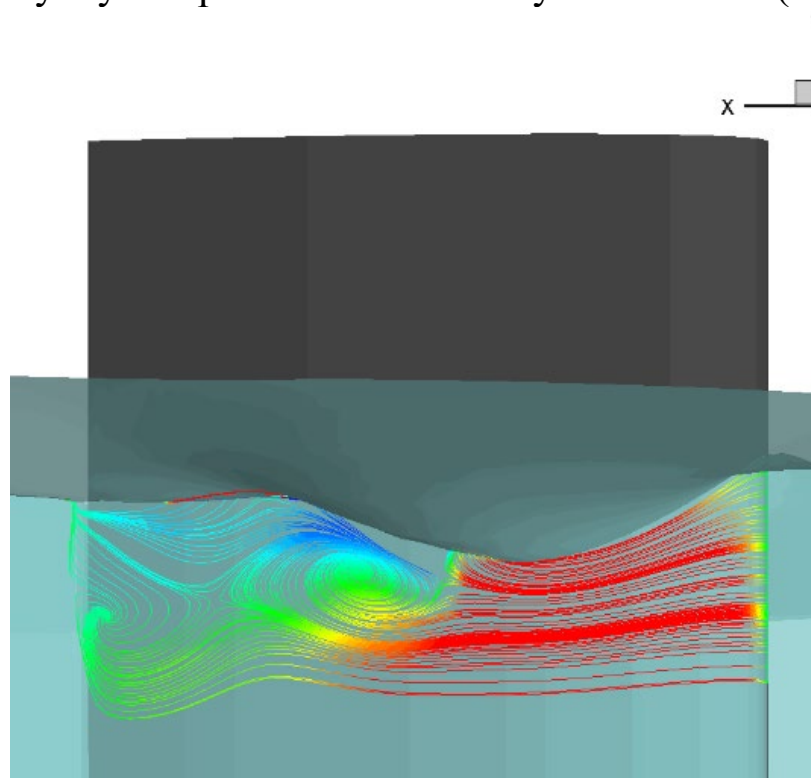
CFDSHIP-IOWA

2. Separation regions in corner flow

FIGURE 4-47
Separation regions in corner flow between airfoils. [*After Gersten* (*1959*).]

3. 3D separations on a round-nosed body at angle of attack

FIGURE 4-49. Three-dimensional separation on a round-nosed body at angle of attack, first described by Legendre (1965). Point A is a nodal attachment point, point S is a saddle point, and point F is a focus of separation.

Video Library (animations from "Multi-media Fluid Mechanics", Homsy, G. M., etc.)
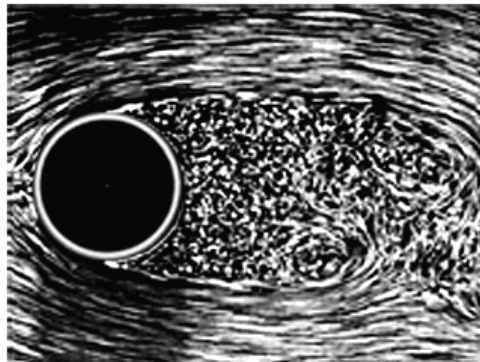

Conditions Producing Separation
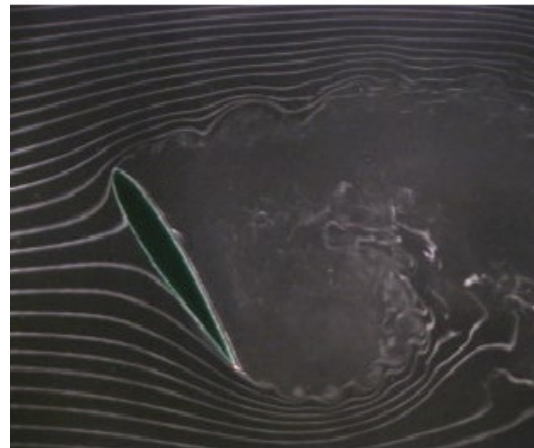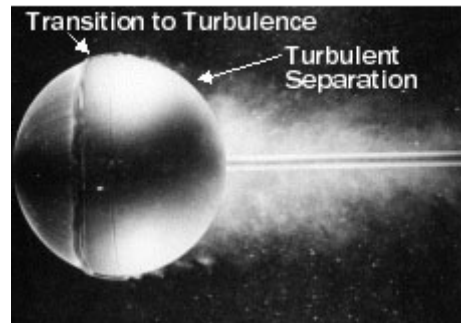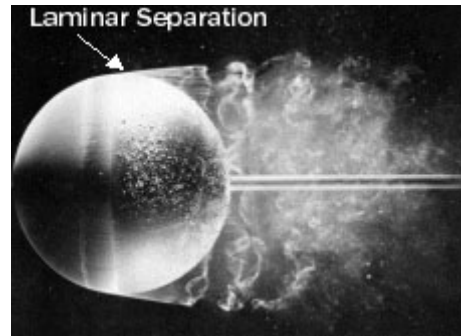

Separations on airfoil (different attack angles)
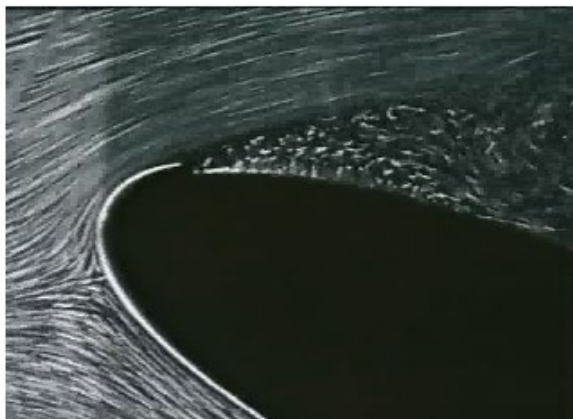
Effect of body shape on separation

Laminar and Turbulent separation
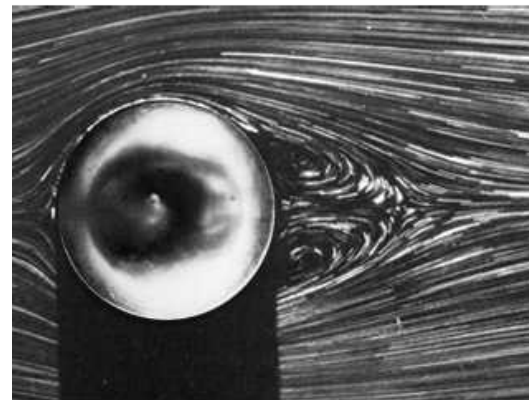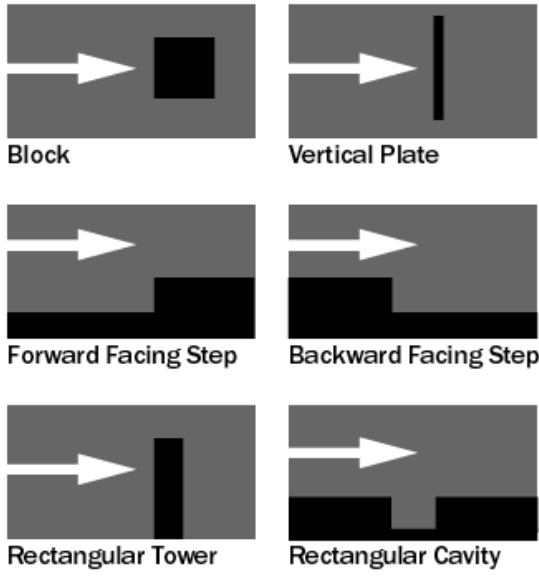
Flow over edges and blunt bodies

Flow over a truck
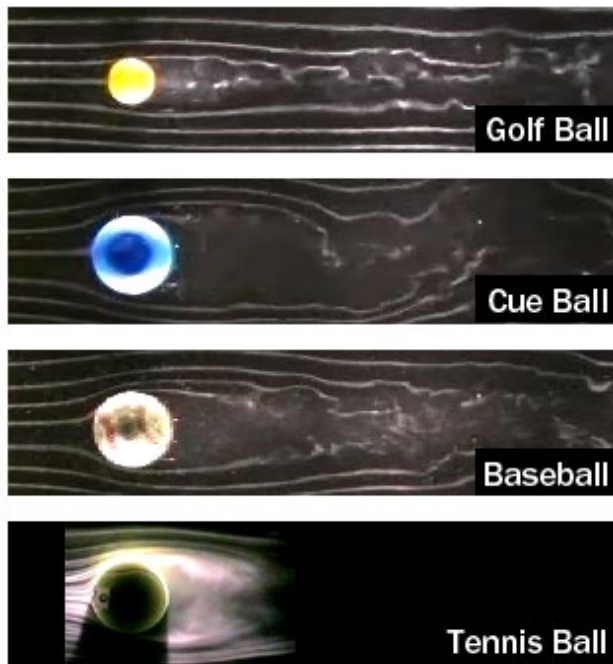
Effect of separation on sports balls